Oxidative dehydrogenation of propane with N2O over Fe-ZSM-5 and Fe-SiO2: Influence of the iron species and acid sites

Ates, A., Hardacre, C., & Goguet, A. (2012). Oxidative dehydrogenation of propane with N2O over Fe-ZSM-5 and Fe-SiO2: Influence of the iron species and acid sites. *Applied Catalysis A: General*, *441*, 30-41. https://doi.org/10.1016/j.apcata.2012.06.038

Published in:
Applied Catalysis A: General

Document Version:
Peer reviewed version

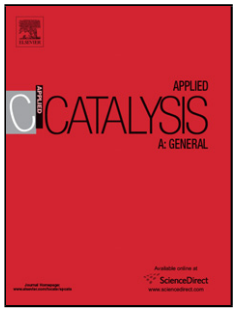

Title: Oxidative Dehydrogenation of Propane with N_2O overFe-ZSM-5 and Fe-SiO_2: Influence of the iron species and acid sites

Authors: Ayten Ates, Christopher Hardacre, Alexandre Goguet

PII: S0926-860X(12)00402-4
DOI: doi:10.1016/j.apcata.2012.06.038
Reference: APCATA 13752

To appear in: *Applied Catalysis A: General*

Received date: 20-2-2012
Revised date: 22-6-2012
Accepted date: 24-6-2012

Please cite this article as: A. Ates, C. Hardacre, A. Goguet, Oxidative Dehydrogenation of Propane with N_2O overFe-ZSM-5 and Fe-SiO_2: Influence of the iron species and acid sites, *Applied Catalysis A, General* (2010), doi:10.1016/j.apcata.2012.06.038

Graphical abstract

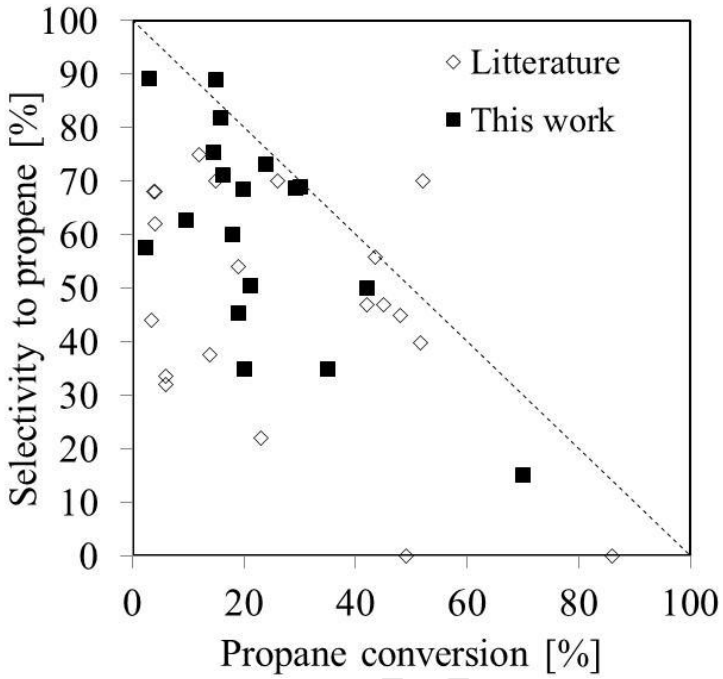

Highlights

Fe-ZSM-5 zeolites prepared with solid-state show high stability for ODHP.

The acidity degree of Fe-ZSM-5 is important for high propene selectivity.

The acidity of Fe-ZSM-5 can be controlled by the treatment conditions and Si/Al ratio.

Highly selective propane dehydrogenation to propene over Fe- SiO_2 is obtained.

Oxidative Dehydrogenation of Propane with N_2O over Fe-ZSM-5 and Fe-SiO_2: Influence of the iron species and acid sites

Ayten Ates*[a], Christopher Hardacre[b] and Alexandre Goguet[b]

[a]Cumhuriyet University, Engineering Faculty, Department of Chemical Engineering, 58140 Sivas, Turkey. E-mail: ates@cumhuriyet.edu.tr; Tel: +903462191010/2248; Fax:+903462191179

[b]School of Chemistry and Chemical Engineering, Queen's University Belfast, Belfast BT9 5AG, Northern Ireland. E- mail: c.hardacre@qub.ac.uk., Tel: + 44 28 90 974592; Fax: + 44 28 90 974687; E-mail: a.goguet@qub.ac.uk, Tel: + 44 (0) 28 9097 4882, Fax: + 44 (0) 28 9097 4687.

*Corresponding author current address: Department of Chemical Engineering, Massachusetts Institute of Technology, Cambridge, Massachusetts, US, 02139. [a]E-mail: aates@mit.edu.

Abstract

A series of iron containing zeolites with varying Si/Al ratios (11.5 to 140) and low iron content (~0.9 wt. % Fe) have been synthesised by *solid-state* ion exchange with commercially available zeolites and tested, for the first time, in the oxidative dehydrogenation of propane (ODHP) with N_2O. The samples were characterised by XRD, N_2-Adsorption, NH_3-TPD and DR-UV-vis spectroscopies. The acidity of the Fe-ZSM-5 can be controlled by high temperature and steam treatments and Si/Al ratio. The selectivity and yield of propene were found to be the highest over Fe-ZSM-5 with low Al contents and reduced acidity. The initial propene yield over Fe-ZSM-5 was significantly higher than that of Fe-SiO_2 since the presence of weak and/or medium acid sites together with oligonuclear iron species and iron oxides on the ZSM-5 are found to enhance the N_2O activation. The coking of Fe-ZSM-5 catalysts could also be controlled by reduction of the surface acidity of ZSM-5 and by the use of O_2 in addition to N_2O as the oxidant. Fe-ZSM-5 zeolites prepared with solid-state method have been shown to have comparable activity and better stability towards coking compared with Fe-ZSM-5 zeolites prepared by liquid ion exchange and hydrothermal synthesis methods.

Keywords: Fe-ZSM-5; Dehydrogenation of propane; propene; nitrous oxide; Fe-SiO_2

1. Introduction

ZSM-5 zeolites with low iron contents have shown remarkable activity and selectivity in the oxidative dehydrogenation (ODH) of propane with N_2O [1-10] as well as in the hydroxylation of benzene [11-15] and other hydrocarbons [11, 16, 17]. The activity and selectivity in ODH of propane (ODHP) can be related to the structure of the ZSM-5, the type of oxidant used, the speciation of the iron and the pre-treatment of the catalysts. For example, it is clear that the acid-base properties of the ZSM-5 are important parameters in the performance of these types of catalysts. Nowinska et al. studied the influence of the acid site concentration on the selectivity and conversion of propane and ethane using N_2O as the oxidant over Fe-ZSM-5 prepared by liquid phase ion exchange [9, 10, 17]. A decrease in Brønsted acid sites via high temperature treatment, sodium doping and hydrothermal treatment resulted in an increase in the propene selectivity, a slight change in the distribution of the cracking products as well as a decrease in the alkane conversion. In the presence of strong acid sites, both dehydrogenation and cracking reactions were reported to occur simultaneously whereas over medium/weak acid sites, the process was found to occur via consecutive reactions. Teixeira-Neto et al. and Bandiera et al. reported that, while the C-H bond of propane is primarily activated on weak and medium acid sites and results in the production of olefins, C-C bonds are primarily activated on strong acid sites and lead to the production of cracking products [18, 19]. In order to reduce the concentration of strong acid sites, Xu et al. investigated the performance of zeolite based catalysts with a range of Si/Al ratios for the dehydrogenation of propane [20]. They found that the activity in propane dehydrogenation decreased with increasing Si/Al ratio while the opposite trend was observed regarding the catalyst stability. The enhanced stability with increasing Si/Al ratio was linked to the reduced acidity of the catalysts, leading to the

suppression of side reactions such as cracking and oligomerization. In contrast, Perez-Ramirez and Gallardo- Llamas reported that the initial propene yield over Fe-ZSM-5 and Fe-BEA prepared by hydrothermal synthesis was not affected by the catalyst acidity, the distribution of extraframework iron species or the zeolite structure [6]. They also reported that Fe-AlMFI and Fe-GaMFI had significantly higher stability in comparison to Fe-GeMFI and Fe-MFI with the former having 2- 3 times higher acid site density [7]. The differences observed between the acidity and ODHP performance of Fe-ZSM-5 zeolites prepared by hydrothermal synthesis or liquid ion exchange may be due to the types of iron species formed in each case and the nature of the pre-treatments used, as discussed below.

Fe-ZSM-5 prepared by methods leading to extra-framework iron led to catalysts having higher activity for N_2O decomposition and higher initial activity for ODH of propane with N_2O compared with other methods of preparation. These materials also showed lower resistance to deactivation. The high initial activity may be due to the presence of isolated and oligonuclear iron species in the extra-framework iron catalysts [21-24]. It has been proposed that the low stability could be improved by increasing the acidity [7] in contrast to ion exchange methods. Catalysts prepared by the solid-state iron exchange method, as studied in detail by Lobree et al. [25] have different active iron species such as large oxide clusters and small oxygen containing nanoclusters such as Fe_4O_4 and Fe_3O_4 [25-28] as well as isolated iron species. They reported that Fe^{3+} cations are exchanged with protons at the Brønsted acid sites on a one-to-one basis for an Fe/Al ratio of 0.56 and formed dispersed cations such as $Fe(OH)^{2+}$, $Fe(OH)^{+}$ and FeO^{+}. Additionally, Abu-Zied et al. reported that the solid- state ion exchange method has various advantages compared with other methods, such as the control of the metal loading, the possibility of exchanging multivalent cations

into the zeolite, the reproducibility, the control of crystallite size and the generation of different active sites [29].

The pre-treatment conditions have also been reported to have a significant effect on the activity and selectivity for the ODH of propane with N_2O. These conditions have included high temperature calcination and/or steaming [3, 4, 9, 10, 21-23, 30]. The high temperature treatment and steaming have been reported to increase the amount of extra-framework iron species in Fe-ZSM-5 prepared by hydrothermal method. It has also been reported that the high temperature treatments increased the activity for N_2O decomposition and ODH of propane with N_2O of Fe-ZSM-5 catalysts prepared by ion exchange [4, 30, 31].

The type and concentration of oxidants have also been reported to affect the activity and selectivity of Fe-ZSM-5. Monoatomic oxygen species (O^{2-}, Oα, O^-) are formed upon N_2O activation, while polyatomic oxygen species ($(O_2)_s$, $(O_2^-)_s$, $(O_2^{2-})_s$) as well as monoatomic species are formed from O_2 activation [32]. The O^- and/or monoatomic oxygen have been reported to be responsible for the ODH of propane over the iron species [4-6]. Nowinska et al. proposed that, upon N_2O decomposition, the surface oxygen formed is responsible for the production of oxygenates such as acetaldehyde [4]. Perez-Ramirez et al. suggested that the monoatomic oxygen species are involved in the conversion of propane to propene [5, 6].

While Fe-ZSM-5 catalysts prepared by hydrothermal or ion exchange methods have been studied extensively for the ODH with N_2O reaction, similar catalysts prepared by solid-state exchange have only been the subject of a limited number of investigations. To the best of our knowledge, alkane dehydrogenation reactions have only been reported using Zn, Mo and Co modified ZSM-5 catalysts prepared by solid state methods [33]. In this case, propane aromatization was reported and demonstrated that highly active catalysts

could be formed via solid-state exchange. The present study compares, for the first time, a series of iron containing zeolites with varying Si/Al ratios (11.5 to 140) and low iron content (~0.9 wt. % Fe) synthesised by solid-state ion exchange using commercially available zeolites for the dehydrogenation of propane following low temperature, high temperature or steam treatments. All catalysts were characterised by XRD, N_2-Adsorption, NH_3-TPD and DR-UV-vis spectroscopies in order to determine the impact of the various treatment and the Si/Al ratio on the nature of the iron species present and the acidity of these catalysts and clarify their impact on the activity and selectivity for ODHP.

2. Experimental

2.1. Catalysts preparation

A range of parent zeolites (NH_4-ZSM-5) with varying Si/Al ratio were used in this study (Zeoliyst, Z: CBV2314, Si/Al=11.5; CBV3024E, Si/Al=15.0; CBV5524G, Si/Al=25.0; CBV8014, Si/Al=40.0; CBV28014, Si/Al=140; Süd-Chemie, SM27, Si/Al=12.5). A series of Fe/SiO_2 reference catalysts were also prepared. The silica support was obtained from Merck (medium pore size: 60 ˚A, particle size: 0.063-0.200 mm). The pre-treatment of the silica and the deposition of the iron were undertaken using the procedures described by Ananieve and Reitzmann [34].

The iron was deposited on all the zeolites by a solid-state technique using $FeCl_2.4H_2O$ as the iron precursor at atmospheric pressure and 550 ^oC, as described elsewhere [31]. The ammonia form of the zeolites was mixed with the iron precursor using a mortar and pestle under ambient conditions. All the samples had a nominal iron loading of 1.0 wt.%. The physical mixture was heated up to 550 ^oC over 3 h and maintained at this temperature in air

for 6 h. Thereafter, the samples were cooled to room temperature, washed thoroughly with deionised water, dried at 120 ^{o}C and calcined at 600 ^{o}C in air for 1 h. The samples are denoted as follows throughout the text: SM*x*Fe*y* or Z*x*Fe*y*, where SM and Z denote the zeolite supplier (Z: Zeoliyst and SM: Süd-Chemie) and *x* and *y* indicate the SiO_2/Al_2O_3 ratio and wt.% of Fe, respectively. The Fe-SiO_2 catalysts were prepared by wet impregnation of the silica support with a solution of Fe(III) acetylacetonate (Aldrich) in toluene at ambient temperature and atmospheric pressure for 15 h. The solvent was then evaporated and the sample was dried and calcined in air at 600 ^{o}C for 5 h. Three Fe-SiO_2 catalysts were prepared by this method with iron contents of 0.1, 0.67 and 0.90 wt.%. Before testing, the iron loaded silica was shaped by extrusion with Ludox (AS-40, Du Pont) and hydroxyl-ethylene-cellulose and the resulting extrudates were crushed and sieved to 250-500 μm particles.

2.2. Characterisation of the catalysts

The chemical composition of the catalysts was measured using ICP. Powder X-ray diffraction (XRD) was performed on a PANalytical X'Pert Pro X-ray diffractrometer using Cu Kα radiation, with a 0.017° step size at room temperature and the spectra were recorded over a 2θ range of 5-65^{o}. Diffuse reflectance ultraviolet-visible spectroscopy (DR-UV-vis) measurements were performed at 30 ^{o}C and 400 ^{o}C after each treatment, using a Lambda 650S UV-vis spectrophotometer equipped with a Harrick high temperature reaction chamber and an integrating sphere detector. The parent zeolites and the silica support were used as reference. The BET surface areas of the samples were measured with an Autosorb 1C, Quantachrome gas sorption apparatus.

Low temperature (LT), steam (ST) and high temperature (HT) treatments were performed at 500 ^{o}C in He (LT) for 2 h, at 600 ^{o}C in 30 % H_2O in He for 5 h (ST) and at 900 ^{o}C in He for 2 h (HT), respectively. Additionally, to explore the combined effect of treatments the samples were treated at HT for 2 h after the ST, and denoted as STHT.

Ammonia temperature-programmed desorption (TPD-NH_3) was carried out in an Autochem II- 2920, Micromeritics. Typically, the samples were saturated with a flow of 15% NH_3 in He at 50 ^{o}C. Subsequently, NH_3 was desorbed in a He flow of 25 cm^3 min^{-1} using a ramp rate of 10 ^{o}C min^{-1} up to a temperature of 700 ^{o}C.

Thermogravimetric (TG) measurements were performed in a TGA-50 apparatus (Shimadzu). These ex-situ measurements allowed analyzing the amount of coke deposited on the samples during long term ODH of propane tests (415 min). Typically, these measurements were performed in a flow of air with a maximum of 10 mg of samples and a temperature ramp rate of 10 ^{o}C min^{-1} from ambient temperature to 900 ^{o}C.

2.3. Catalytic tests

The ODHP with N_2O was carried out in a fixed bed reactor (i.d.=20 mm) at atmospheric pressure. The amount of catalyst used was 0.5 g. The feed composition was 5% N_2O and 5% C_3H_8 in He with a total flow rate of 200 cm^3 min^{-1} unless otherwise stated. All experiments were performed at 450 or 500 ^{o}C. Before the ODHP activity tests, the samples were pre-treated using the LT, ST, HT or STHT conditions. For the long term ODHP activity tests and the subsequent evaluation of the amount of coke deposited, the experiments were conducted for 415 min and the products analysed every 20 min. For all ODHP tests, the reactants and products were analysed by on-line gas chromatography (Agilent 2920) equipped with both a TCD and a FID detector. Plot Q and Molsieve 3A

columns were used to separate N_2, O_2 and N_2O and an Al/S column was used to separate the organic compounds such as methane, ethane, propane and propene. The conversion (X), yield (Y) and selectivity (S) were calculated using the following equations:

$$X_{C3H8} = (C^{o}_{C3H8} - C_{C3H8}) / C^{o}_{C3H8} \quad (2.1)$$

$$X_{N2O} = (C^{o}_{N2O} - C_{N2O}) / C^{o}_{N2O} \quad (2.2)$$

$$Y_{C3H6} = C_{C3H6} / C^{o}_{C3H8} \quad (2.3)$$

$$S_{C3H6} = Y_{C3H6} / X_{C3H8} \quad (2.4)$$

where C_i^o and C_i refer to the input and output concentrations of species mol/L, respectively.

3. Results

3.1. Characterisation of the catalysts

Chemical composition and X-ray diffraction

Table 1 reports the chemical composition of the Fe–ZSM-5 and Fe-SiO_2 catalysts determined by ICP. Some differences from the nominal loadings were found. Similar differences have been reported previously [29, 30] and have been tentatively attributed to HCl formed in the washing step during preparation causing a loss of iron and/or aluminium. In the case of the Fe-SiO_2 catalysts, the measured iron contents were close to the theoretical amounts.

The XRD patterns for the Fe-ZSM-5 samples as a function of the various thermal treatments were measured (not shown). Neither LT nor HT treatments significantly affected the zeolite crystallinity. Conversely, following ST, a significant reduction in the

intensity of the XRD peaks was observed which is consistent with de-alumination of the zeolite [12,14]. In all cases, for both zeolite and silica samples, little change in the XRD patterns were observed between the parent zeolite and the iron loaded sample.

Nitrogen adsorption

The textural properties of the samples after LT, HT and ST treatments were investigated by nitrogen adsorption. The isotherms obtained for all zeolite samples were of Type I as expected for microporous solids [35]. The specific surface area, pore volumes and average pore diameters for the fresh and treated samples are reported in Table 2. Almost all Fe-ZSM-5 samples treated at HT showed a decrease in BET area, pore volume and average diameter of the micropores (Table 2) which is likely to be due to the aggregation of iron species in the micropores. After LT and HT treatment, the hysteresis between adsorption and desorption for $p/p^o > 0.5$ became much less significant indicating the very small contribution of the mesoporosity to the overall porosity of the treated samples. After the ST treatment, the N_2 uptake for the samples did not change significantly. A hysteresis between adsorption and desorption isotherms of N_2 in Fe-SiO_2 (not shown) indicated the presence of mesopores, as expected for silica. Overall, the deposition of the iron resulted in only small modifications of the BET isotherm profiles.

DR-UV-vis spectroscopy

Figure 1 shows the DR-UV-vis spectra of the Fe-ZSM-5 samples after the LT, HT and ST treatments. For similar catalysts reported previously, bands at 230 nm, 250 nm, 270 nm, 338 nm and above 400 nm have been observed [13, 22, 36-39]. Perez-Ramirez et al.

identified three spectral regions corresponding to bands at wavelengths <300 nm associated with isolated Fe^{3+} ions, bands between 300 and 400 nm ascribed to small oligonuclear $Fe_x^{3+}O_y$ clusters and bands above 400 nm corresponding to Fe_2O_3 nanoparticles on the external surface of the zeolite [22]. Similar assignments have been reported by Centi et al. [12-14] and Berlier et al. [37]. For the Fe-ZSM-5 samples studied, herein, treated at LT (Figure 1a) a feature at ~225 nm was observed for all samples. This is consistent with the presence of isolated Fe^{3+} sites in the tetrahedral coordination. In addition, all the samples displayed broad peaks around 270 nm indicating the presence of isolated iron species in square-pyramidal and distorted octahedral coordination [40]. For samples with low Si/Al ratios (11.5- 25), features were also observed between 300 and 400 nm (a peak for Z30Fe1.0 and shoulders for Z23Fe1.0 and Z50Fe1.0). This indicated the presence of small oligonuclear $Fe_x^{3+}O_y$ clusters. Additionally, all samples displayed broad bands above 450 nm due to the presence of large Fe_2O_3 particles. Figures 1b and c show the DR-UV-vis spectra for the samples after ST and HT treatments, respectively. Both treatments led to a decrease in the intensity of the bands located below 300 nm and the appearance of broad bands above 400 nm due to the sintering of isolated iron species into larger iron oxide species [41]. The DR-UV-vis spectra for the Fe-SiO_2 catalysts are reported in Figure 1d. At low iron loadings, a single band around 270 nm is observed. As the loading of iron is increased an additional band at 300 nm is observed. As expected the increased iron loading leads to the formation of small oligonuclear clusters ($Fe_x^{3+}O_y$) in addition to the isolated iron species which are present at the lower loadings.

NH_3 –TPD

Figure 2 shows the NH_3-TPD profiles obtained for the parent zeolites after LT and HT treatments. Three desorption peaks were observed at 100, 180 and 400 ^oC. The peaks at 100 ^oC and 400 ^oC denote physically and strongly adsorbed ammonia on Brønsted and/or Lewis acid sites, respectively [25, 42-44]. The attribution of the peak at 200 ^oC is more complex. This peak may be due to ammonia weakly adsorbed on Brønsted/ Lewis acid sites [25, 42], ammonia associated with Na^+ [44] or extra-framework Al [42].

For the LT treatment, irrespective of the Si/Al ratio, three desorption peaks were observed for all the parent zeolites with their intensity decreasing with increasing Si/Al ratio. After the HT treatment a strong decrease of the peak at ~400 ^oC was observed for all zeolites which is consistent with a loss of Brønsted acid sites [10]. It is worth noting that the loss of acid sites has been thought to be due to partial dealumination [45]; however, from the XRD (not shown) and BET (Table 2) data little change following HT treatment is observed and, therefore, this is unlikely to be the cause in the present case. The NH_3-TPD profiles of the parent and iron exchanged zeolites after LT treatment (Figure 3) showed that the peak observed at ~400 ^oC with the parent zeolites significantly decreases on iron deposition for samples with a Si/Al ratio of 50 or below. This is likely to be due to the exchange of surface protons by iron cations [25]. At higher Si/Al ratios, the intensity of this peak is either unchanged or smaller, as seen in Figure 3, due to the formation of iron oxides at the lower alumina content. Moreover, at the highest Si/Al ratio (Z280), the peak broadens and behaves similarly to that observed for the pure silica based catalysts reported in Figure 5.

The NH_3-TPD profiles of the different Fe-ZSM-5 samples after LT, ST and HT treatments are similar to those of the parent zeolites (Figure 4). In each case, the peak intensity

decreased following the HT and ST treatments, which is indicative of a significant reduction of the acidity of the samples. The largest change was observed following ST which is consistent with the fact that such treatments result not only in the removal of Brønsted acid sites but also dealuminate the samples. This is consistent with other studies of similar materials and treatments [12, 14, 41].

The NH_3-TPD profiles of the Fe-SiO_2 are provided in Figure 5 and show that the amount of physically adsorbed ammonia increased with increasing iron content while the amount of ammonia desorbed for temperature above 600 ^{o}C follow the opposite trend. This is thought to be due to hydroxylation of the silica at temperatures higher than 600 °C, as reported by Katranas et al. [46], which decreases with increasing iron content.

3.2. Activity results of the catalysts

Oxidative dehydrogenation of propane with N_2O over Fe-ZSM-5

Figure 6 reports the ODHP performance of all Fe-ZSM-5 catalysts at 450 ^{o}C after the LT treatment. The highest initial propane conversion, 40 %, was observed over the Z23Fe1.0 sample, but both the yield and selectivity for propene were low. The highest initial yield, 10%, was obtained over the Z280Fe1.0 sample; however, the conversion and yield decreased with time on stream for samples with high Si/Al ratios. This is not due to coking of the surface with little carbon deposition found as shown in Table 3 and the propene selectivity remained high. It is interesting to note that the highest deactivation rate was also observed in the N_2O conversion. Considering that the N_2O conversions decreased with time whilst the selectivity to propene increased and the propene yield was reasonably constant, it is likely that the deactivation observed is mainly due to the deactivation of the

sites available for the direct decomposition of N_2O. This leads to a reduction in the unwanted combustion reactions, for example, and hence the increase in selectivity observed. For the samples with low Si/Al ratios, methane, ethane, ethylene, butane and carbon dioxide were observed in addition to propene. In all cases the predominant by-products were carbon dioxide and methane with the highest concentrations found for Z23Fe1.0 in the range of 24-30% for CO_2 and 3-7% CH_4. With time on stream, in contrast with the conversion of propane, the yield of CO_2 increased. This is likely due to the conversion of propene or the other by-products such as methane, ethane, ethylene and butane to CO_2 since their concentration decreased with time on stream. These by-products were also observed for the highest Si/Al ratios (i.e. Z80Fe1.0 and Z280Fe1.0), but their concentrations were considerably lower in this case, which is consistent with the results previously reported for other Fe-ZSM-5 catalysts [9, 17].

Direct decomposition of N_2O was performed over Fe-ZSM-5 zeolites treated at LT, ST and HT (not shown here) and decomposition activity changed in the order HT>ST>L T for all Si/Al ratios. Similar experiments were repeated for Z80Fe1.0 and the highest yield of propene was observed over Z80Fe1.0 treated at HT and the highest conversions of N_2O and C_3H_8 were obtained over Fe80Fe1.0 treated at STHT. Therefore, the STHT pretreatment was subsequently systamatically applied to the samples evaulated for the ODH of propane.

Figure 7 reports the ODHP activities after consecutive ST and HT treatments. These led to an increase in both the conversions and selectivities of propane to propene compared with the LT treatment. The highest propane conversion was obtained for Z80Fe1.0 whilst the highest N_2O conversion was observed with Z50Fe1.0. The highest selectivity for propene was obtained for Z280Fe1.0 and the highest yield was obtained with Z23Fe1.0,

respectively. On the basis of these results, no direct correlation between ODHP performances and the Si/Al ratio of the sample could be drawn. It should be noted, however, that the trend obtained in Figure 7 with such treatment is opposite to that obtained with the samples treated at LT and that the stability of the samples toward coking is increased as seen in Figure 7. This may be due to the formation of small oligonuclear $Fe_x^{3+}O_y$ clusters and of large Fe_2O_3 particles following these treatments, as seen in the DR-UV-vis spectra, which are produced as a result of surface defect formation and dealumination. This is consistent with a number of studies which have also shown that such changes in the catalysts increase the ODHP activity [41, 45, 47-49]. The increase in propene yield and selectivity is thought to be strongly dependent on the removal of Brønsted acid sites which are responsible for oligomerization and cracking reactions leading to coking. In addition, the increased stability towards coking can be the result of the decrease in micropore diameter. Perez-Ramirez and Gallardo-Llamas reported that coke precursors either cannot be trapped inside at the pores intersections or oxidised via molecular oxygen formed through recombination of atomic oxygen adsorbed from N_2O, and thereby diffuse easily due to their weak adsorption [6]. This is consistent with the BET results (Table 2) obtained for the catalysts studied, herein.

Based on the thermogravimetric results of the Fe-ZSM-5 samples used in ODHP for 415 min, reported in Table 3, the coke content of zeolites decreases as a function of the treatment applied in the order ST > HT > STHT, which is consistent with the activity results. The reason for the dependence of the coke accumulation on the treatment used can be summarized as follows: (i) decreasing of Brønsted acid sites; (ii) the conversion of inactive irons species to oligonuclear iron species and/or iron oxides and dealumination,

increasing of the molecular oxygen formation which may lead to oxidation of coke; (iii) the elimination of the iron species which are responsible for coking.

ODHP over Fe-SiO_2

Figure 8 reports the ODHP activity results obtained with Fe-SiO_2 catalysts. Clearly, the activity increased with increasing iron content. Compared with the results obtained with the Fe-ZSM-5 samples (irrespective of the Fe loading and Si/Al ratio of the zeolite based catalysts) the ODHP activity over Fe-SiO_2 was found to be much lower. This difference is likely to be due to the type of the iron species present on the silica and the absence of acid sites. Based on DR-UV-vis results, isolated iron species and/or small oligonuclear iron clusters ($Fe_x^{3+}O_y$) exist on both Fe-ZSM5 and Fe-SiO_2 samples. Considering that the non-quantitative aspect of the DR-UV-Vis data it is, therefore, difficult to draw an accurate relationship between the activity and relative proportion and nature of the iron species present. The very high propene selectivity (almost 100%) during the ODH of propane over Fe-SiO_2 may be due to the absence of Al; however, these results need to be noted with caution since they were obtained at low conversion, the selectivity is likely to decrease with increasing conversion. Keeping this aspect in mind, and assuming that the contribution of Al is real, one could be tempted to introduce aluminium into the silica matrix in order to increase the activity for ODHP of such catalysts. However, in this case the resulting increase in the concentration of acid sites, while likely to improve the ODH activity, will also enhance the cracking of propane. It is for this reason that Perez- Ramirez and Gallardo–Llamas [6] reduced the Brønsted and Lewis acid sites of the zeolites studied, therein, via steaming after introduction of Al.

The influence of the oxidant on ODHP performance

N_2O for ODHP over Fe-ZSM-5 zeolites is a more selective but less active oxidant as compared with molecular oxygen [4]. Recently, Bulánek and Novoveská reported the three-fold higher yield of propene over CoH-BEA zeolite by addition of nitrous oxide to oxygen [2]. This is explained by a synergetic effect of oxygen and nitrous oxide. Although this effect has not been fully explained it is likely to be due to the activation of O_2 and N_2O on different iron species. Therefore, in order to optimize the performance of the present catalysts, the impact of the composition of the feed in terms of the oxidant composition has been explored. Table 4 summarises the propane conversion and propene yield and selectivity for the zeolite (LT) and silica based iron catalysts at 450 and 500 °C using different feed mixtures in terms of $C_3H_8/N_2O/O_2$. Comparing all the zeolite based catalysts using 5% propane + 5% nitrous oxide, the highest propene yield and propane conversion were observed over Z280Fe1.0. However, using 5% propane + 5% oxygen, a decrease in both the yield and conversion was observed for both Z280Fe1.0 and Z80Fe1.0 with the activity over Z80Fe1.0 found to be slightly higher than that over Z280Fe1.0. Using a 1:1 mixture of O_2 and N_2O also resulted in a decrease in the conversion of propane as well as the yield of propene in comparison with pure N_2O as the oxidant, albeit much smaller than when pure O_2 was used. Significant increases in both yield and conversion were observed, however, on increasing the N_2O concentration by a factor of two in the absence of O_2 over Z80Fe1.0.

The results over the zeolite based catalysts are in contrast with those obtained over the silica based materials. In this case, the highest conversion of propane and yield of propene over Fe-SiO_2 were observed when a mixture of N_2O and O_2 was used, albeit still much smaller than virtually all the conditions used for the zeolite catalysts.

The results show that N_2O activation on Fe-ZSM-5 is possible while both O_2 and N_2O activation on Fe-SiO_2 can be achieved. Previous studies showed that the O^- and/ or monoatomic oxygen is responsible for the ODHP over the iron species [4-6]. According to the reports of Panov et al, the O^- and/ or monoatomic oxygen can originate from both O_2 and N_2O [21]. The percentage of these oxygen species is high on iron containing zeolites using N_2O as the oxidant. Whereas O_2 and N_2O can activate on the oligonuclear iron species and larger iron oxides formed in silica and/or zeolites, the presence of acid sites (weak and medium) along with these iron species can enhance N_2O activation as seen in Fe-ZSM-5 with low alumina content and treated in HT and ST.

In relation to the catalyst performance, the highest propene yield was 20% over the Z80Fe1.0 for N_2O:C_3H_8:2:1 and 7.0% over $FeSiO_2$-3 for N_2O:O_2:C_3H_8=1:1:1. Furthermore, the propene selectivity over $FeSiO_2$ was high. This may be due to the absence of strong Brønsted acid sites for these catalysts.

4. Discussion

The performance of Fe-ZSM-5 zeolites on ODH of propane depends on the Si/Al ratio of zeolite, the iron species formed in the zeolite, their pre-treatment conditions and type and concentration of oxidant. Except for the case of Z280, increasing the Si/Al ratio led to a decrease in the initial conversion of propane and nitrous oxide and an increase in the initial selectivity of propane, but without a clear tend between the impact observed and the Si/Al value. Such behaviour may be associated with an increase in the cracking activity of different zeolites with increasing acidity (i.e Al content) as observed with the NH_3-TPD results. With time on stream, a decrease in the conversion of propane and nitrous oxide is

observed, which is most prominent at the lower Si/Al ratios. Similar results were reported by Held et al. [17] for the dehydrogenation of ethane with N_2O. While high conversion of ethane and low selectivity of ethylene were observed for Si/Al of 25 and 50, an opposite result was obtained when the Si/Al was 100. The low selectivity for ethylene in case of the Si/Al of 25 and 50 was related to the presence of high acidic centres (Brønsted or Lewis sites) determined by NH_3-TPD.

Interestingly, while steam and high temperature treatments led to a significant increase in the ODH activity of propane of the iron containing zeolite catalysts explored in this study, it did not adversely affect their stability. Based on the NH_3-TPD and DR-UV-vis results, these improvements with such treatments are likely to be the result of not only a decrease in Brønsted/Lewis acidy but also in the transformation of iron species introduced into the zeolites. Numerous studies have attempted to explain what happen during the treatment at high temperatures and/or steaming treatments for Fe-ZSM-5 zeolites prepared with different methods (hydrothermal method, ion exchange and CVD) for ODH of propane and decomposition of N_2O in literature and discussed by the impact of treatments by various groups. Based on the characterisation results from this study and previous results, it may be proposed that high temperature treatments lead to redispersion of iron oxide clusters [30, 50, 51], the formation of small iron oxide clusters such as –Fe-O-Al like species and isolated Fe^{2+} species [48, 50, 52-54], the creation of hydroxyl nests by dealumination [12, 14], the formation of mono and bi/oligonuclear iron [24], the migration of iron ions located on the outer surface into the pore system [10] and the conversion of Fe^{3+} to Fe^{2+} [55, 56].

Clearly, the NH_3-TPD results showed that the concentration of Brønsted and/or Lewis acid sites of the zeolite catalysts could be reduced by the introduction of iron, the increase of Si/Al ratio and the high temperature and steam treatments. The relationship between iron

introduction and acid sites was reported in our previous study of the decomposition of N_2O over Fe-ZSM-5 zeolites containing varying iron contents and Si/Al ratios [57] which demonstrated that the formation of active iron species necessitates the presence of an optimal Si/Al ratio. This ratio is not important for lower iron loaded catalysts (Fe≤3.30 wt %) because Fe^{3+} cations for an Fe/Al ratio of 0.56 are exchanged with the protons of the Brønsted acid sites on a one-to-one basis and formed dispersed cations such as $Fe(OH)^{2+}$, $Fe(OH)^{+}$ and FeO^{+} [25].

In case of zeolite catalysts prepared by solid-state exchange of iron and containing low Si/Al ratio(Si/Al≤50) a reduced HT peak as compared with the protonic form is observed in the NH_3-TPD profile (Figure 3). The decrease of the HT peak area corresponds approximately to a compensation of negative charges in the zeolite on a 1:1 basis probably due to the incorporation of the cationic iron precursors. However, the total amount of NH_3 desorbed from the Z80 and Z280 samples is not significantly affected by the presence of iron species. This was unexpected when assuming a compensation of negative charges by iron cations as in the case of lower Si/Al ratios. Although NH_3-TPD is known not to be highly quantitative, in the present case quantifying the influence of iron exchange on the number of Brønsted sites in zeolites, Lobree et al. have shown that results of NH_3-TPD experiments correaltes well with the number of bridged hydroxyl groups determined by FTIR for a ZSM5 zeolite (Si/Al = 27) exchanged with different amounts of $FeCl_3$ [25]. Both characterisation methods have shown that iron cations can replace up to approximately 60% of the Brønsted acid protons. In addition, an introduction of iron into lattice defects forming Brønsted sites is also possible, particularly for zeolites with higher Si/Al ratio, as shown by El-Malki et al. using a variety of characterization techniques [58]. This means for the present study that the compensation of Brønsted acid protons by iron

cations can only be detected in NH_3-TPD when isolated cations are present, as for Z23, Z30 and Z50 with low iron contents. At higher Si/Al ratios, the formation of bi- and oligonuclear iron oxo/ hydroxo-species are formed on the surface as well as isolated iron species.

High temperature and steam treatments led to a decrease the total concentration of acid sites and transformation of iron species as seen in Figures 1 and 4. In particular, a significant decrease in the acid concentration was observed after steam treatment of the Fe-ZSM-5, likely due to the fact that steam treatment also induces extensive dealumination of the zeolite and decrease the density of Brønsted acidic sites. This was supported by both XRD and NH_3-TPD results presented, herein. A similar behaviour after steaming were observed by various groups [41,48, 59]. Additionally, DR-UV-vis results showed that the steam treatment increases the concentration of oligonuclear iron species and highly dispersed iron oxide nanoparticles of 1–2 nm in the zeolites.

The decrease in acid sites seems to be linked to a change in the product distribution as well as the conversions of propane and nitrous oxide and selectivity to propene. For example, the selectivity of cracking products is decreased. As stated in the introduction, this can be explained by the fact that only medium and weak acidic sites are responsible for the C-H bond activation, involved in oxidative dehydrogenation pathway [18, 19]. This is supported by the work of Held et al. who reported that the reduction of acid sites by means of high temperature treatment and sodium introduction, results in a clear decrease in selectivity to cracking products and CO_2, while selectivity towards propene increased [10]. Additionally, Held et al. [9] and Bulanek et al. [3] showed that strong acidic sites gave rise to simultaneous formation of ODH and cracking of propane. According to literature data [60-62] the propene formed may undergo dimerization in the presence of medium and weak acidic centres and then can be further converted to shorter hydrocarbons through

cracking. This behaviour may explain why, in addition to CO_2, various hydrocarbons such as methane, ethylene, ethane and butane are observed as a by-products. Interestingly, the concentration of these by products is higher at the beginning of the reaction over Fe-ZSM-5 zeolites with low Si/Al ratio and treated at low temperatures. In such cases, methane and ethane should be mostly formed from cracking of propane. Ethylene could be formed the oxidative dehydrogenation of ethane [10, 17, 62], while butane may be formed by oligomerization of ethylene on the Fe-ZSM-5 zeolites as reported by Amin and Anggoro [63]. CO_2 can be formed from methane, ethylene, ethane, and butane as well as propane and propylene total combustion [10, 17, 62, 63].

Compared with the Fe-ZSM-5 catalysts, Fe-SiO_2 catalysts showed lower propane conversion and higher propene selectivity. As highlighted previously, a direct comparison is difficult since conversion was much lower than the zeolite based catalysts which is known to influence positively the selectivity figures. Keeping these aspect in mind several observation can be made, the activity differences may be due to the presence of Al in the zeolite based catalysts as well as different iron species formed in the different samples. In case of the different iron species, based on DR-UV-vis results, both samples contain small oligonuclear clusters ($Fe_x^{3+}O_y$) and isolated iron species as well as iron oxide nanoparticles of 1-2 nm. Therefore, it is difficult to find a relationship between iron species and the activity forthe ODH of propane. However, the presence of Al on Fe-ZSM-5 (possibly in the form of Fe-O-Al) can enhance the activation of propane and nitrous oxide as reported by Hensen et al. [52, 53].

The activity and selectivity of ODHP strongly depends on the nature of the oxidant used. Propane mainly converts to propene with N_2O and O_2 over Fe-ZSM-5 and Fe-SiO_2. Moreover, the use of O_2 as the oxidant reduced the coke content, as seen in Table 3, and,

therefore, this may indicate that the polyatomic oxygen species formed from O_2 oxidise the coke precursors. As reported by Perez-Ramirez and Gallarda-Llamas for ODHP [6, 7] and Pirutko et al. [64] for the direct oxidation of benzene to phenol (BTOP), the presence of Brønsted acidity in the zeolites activates iron species responsible for these reactions. As already stated [18, 19], the selectivity and yield of propene is high on the zeolites with lower Al content and with acidity reduced via HT and ST treatments, leading to weak and medium acid sites responsible for the activation of the C-H bond of propane.

ODHP has been studied previously on Fe-ZSM-5 prepared using hydrothermal or ion exchange methods. The highest values for conversion of propane and selectivity and yield of propene were observed for Fe-ZSM-5 zeolites prepared with hydrothermal method and using N_2O and N_2O+O_2 as the oxidant [3, 6, 7]. However, a drawback of these methods is the rapid deactivation of the catalysts. Perez Ramirez and Galarda – Llamas were able to stabilise the activity through introduction of Ga and Al into the zeolite [7]. Although Fe-ZSM-5 zeolites prepared with ion exchange by Nowinska et al. showed comparable propene yield (22 %) using Fe-ZSM-5 treated at 900 ^{o}C compared with the hydrothermally prepared catalysts, the selectivity to propene and the conversion of propane were lower than that obtain with hydrothermal methods [4]. Figure 9 reports the conversion-selectivity plot of the best results obtained with our catalysts and those reported previously for Fe-ZSM-5 catalysts using similar conditions [2-5, 8, 10]. As expected, all the points (with only one exception) were located on the lower left hand size of the line linking the 100% conversion and 100% selectivity poles. Moreover, the general trend of the results obtained was that of a decreasing propene selectivity with increasing propane conversion, which is the most commonly obtained trend in case of alkanes partial oxidation. Comparing these results with those previously reported, the representative points are

reasonably close to the "100% conversion and 100% selectivity" separation line. It is, therefore, reasonable to conclude that the Fe-ZSM-5 zeolites prepared, herein, by the solid-state method have comparable performance with Fe-ZSM-5 zeolites prepared with hydrothermal method and, most interestingly, stability towards coking as seen in Figure 7.

5. Conclusions

The ODH of propane on Fe-ZSM-5 prepared by solid-state methods as well as using Fe-SiO_2 has been examined in detail, for the first time. In particular, the effect of low temperature, high temperature and steam treatments on materials prepared by this method have been examined. Importantly, Fe-ZSM-5 zeolites prepared with solid-state method have been shown to have comparable activity and better stability towards coking compared with Fe-ZSM-5 zeolites prepared by hydrothermal synthesis. In addition, the acidity of Fe-ZSM-5 which is shown to be important towards the ODH performance of these catalysts can be controlled by high temperature and steam treatments and Si/Al ratio. In order to obtain high selectivity towards propene, the presence of weak and medium acid sites is necessary which can be obtained by steam and high temperature treatments as well as changes in the Si/Al ratio. The steam treatment was found to lead to dealumination of the zeolites and aggregation of the iron species. Based on DR-UV-vis data, the cationic iron species can be converted into oxidic iron species and oligonuclear iron species via the steam treatment leading to an increase in conversion of propane conversion. Similar results were also found after a high temperature treatment.

Acknowledgements

The authors acknowledge financial support from the Scientific and Technological Research Council of Turkey (107M236) and the EU Transnational Project grant held in CenTACat at Queen's University, Belfast.

References

[1] R. Bulanek, K. Novoveska, B. Wichterlova, Appl. Catal. A 235(2002) 181-191.

[2] R. Bulanek, K. Novoveska, Reac. Kint. Catal. Lett. 80 (2003) 337-343.

[3] R. Bulanek, B. Wichterlova, K. Novoveska, V. Kreibich Appl. Catal. A 264 (2004) 13-22.

[4] K. Nowinska, A. Waclaw A. Izbinska, Appl. Catal. A 243 (2003) 225-236.

[5] E. V. Kondratenko, J. Perez- Ramirez, Appl. Catal. A 267 (2004) 181-189.

[6] J. Perez-Ramirez, A. Gallardo-Llamas, J. Catal. 223 (2004) 382-388.

[7] J. Perez-Ramirez, A. Gallardo-Llamas, J. Phys. Chem. B 109 (2005) 20529-20538

[8] A. Gallardo- Llamas, C. Mirodatos, J. Perez- Ramirez, Ind . Eng. Chem. Res. 44 (2005) 455-462.

[9] A. Held, J. Kowalska, A. Tuchorska, K. Nowinska, Stud. Surf. Sci. Catal. 170 (2007) 1267-1274.

[10] J. Kowalska-Kus, A. Held, K. Nowinska, Catal. Lett. 136 (2010) 199-208.

[11] V. I. Sobolev, K. A. Dubkov, O. V. Panna, G. I. Panov, Catal. Today 24 (1995) 251-252.

[12] G. Centi, C. Genovese, G. Giordano, A. Katovic, S. Perathoner, Catal. Today 91/92 (2004) 17-26.

[13] G. Centi, S. Perathoner, F. Pino, R. Arrigo, G. Giordano, A. Katovic, V. Pedulà, Catal. Today 110 (2005) 211-220.

[14] G. Centi, S. Perathoner, R. Arrigo, G. Giordano, A. Katovic, V. Pedula, Appl. Catal. A 307 (2006) 30-41.

[15] T. Tatlier, L. Kiwi-Minsker, Catal. Commun. 6 (2005) 731-736.

[16] M. A. Rodkin, V.I. Sobolev, K. A. Dubkov, N. H. Watkins, G. I. Panov, Stud. Surf. Sci. Catal. 130 (2000) 875-880.

[17] A. Held, J. Kowalska, K. Nowinska, Appl. Catal. B 64 (2006) 201-208.

[18] J. Bandiera, M. Dufaux, Y. B. Taarit, Appl. Catal. B 148 (1997) 283-300.

[19] A. A. Teixeira- Neto, L. Marchese, G. Landi, L. Lisi, H. O. Pastore, Catal. Today 133–135 1(2008) 1-6.

[20] B. Xu, T. Li, B. Zheng, W. Hua, Y. Yue, Z. Gao, Catal. Lett. 119 (2007) 283-288.

[21] J. Perez-Ramirez, E. V. Kondratenko, Chemm. Commun. (2003) 2152-2153.

[22]J. Perez-Ramirez, M. S. Kumar, A. Brückner, J. Catal. 223 (2004) 13-27.

[23] J. Perez-Ramirez, J. G. Groen, A. Brückner, M. S. Kumar, U. Bentrup, M. N. Debbagh, L. A. Villaescusa, J. Catal. 332 (2005) 318-334.

[24] I. Yuranov, D. A. Bulushev, A. Renken, L. Kiwi-Minsker, J. Catal. 227 (2004) 138-147.

[25] L. J. Lobree, I. C. Hwang, J. A. Reimer, A.T. Bell, J. Catal. 186 (1999) 242-253.

[26] R. Joyner, M. Stockenhuber, J. Phys. Chem. B 103 (1999) 5963-5976

[27] E. M. El-Malki, R. A. Van Santen, V. M. H. Sachtler, J. Catal. 196 (2000) 212-223.

[28] B. R. Wood, J. A. Reimer, A. T. Bell, J. Catal. 209 (2002) 151-158.

[29] B. M. Abu- Zeid, W. Schwieger, A. Unger, Appl. Catal. B 84 (2008) 277-288.

[30] A. Waclaw, K. Nowinska, W. Schwieger, A. Zielinska, Catal. Today 90 (2004) 21-25.

[31] M. Kögel, R. Mönnig, W. Schwieger, A. Tissler, T. Turek, J. Catal. 182 (1999) 470-478.

[32] G. I. Panov, K. A. Dubkov, E. V. Starokon, Catal. Today 117 (2006) 148-155.

[33] Z. Fu, D. Yin, Y. Yang, X. Guo, Appl. Catal. A 124 (1995) 59-71.

[34] E. Ananieve, A. Reitzmann, Chem. Eng. Sci. 59 (2004) 5509-5517.

[35] K. S.W. Sing, D. H. Everett, R. A.W. Haul, L. Moscou, R.A. Pierotti, J. Rouquerol, T. Siemieniewska, Pure Appl. Chem. 57 (1985) 603-619.

[36] J. H. Park, J. Choung, I. S. Nam, S.W. Ham, Appl. Catal. B 78 (2008) 342-354

[37] G. Berlier, G. Ricchiardi, S. Bordiga, A. Zecchina, J. Catal. 229 (2005) 127-135.

[38] M. S. Kumar, M. Schwidder, W. Grünert, A. Brückner, J. Catal. 227 (2004) 384-397.

[39] S. Bordiga, R. Buzzoni, F. Geobaldo, C. Lamberti, E. Giamello, A. Zecchina, G. G. Leofanti, G. Petrini, G. Tozzola, G. Vlaic, J. Catal. 158 (1996) 486-501.

[40] G. Lehmann, Z. Phys. Chem. Neue Folge 72 (1970) 279-297.

[41] Q. Zhu, B. I. Mojet , R. A. J. Janssen , E. J. M. Hensen, J. van Grondella, P. C. M. M. Magusin, R. A. van Santen, Catal. Lett. 81 (2002) 205-212.

[42] G. I. Kapustin, T. R. Brueva, A. L. Klyachko, S. Beran, B. Wichterlova, Appl. Catal. 42 (1988) 2239-246

[43] I. Melian-Cabrera, S. Espinosa, J. C. Groen, B. van der Linden, F. Kapteijn, J.A. Moulijn, J. Catal. 238 (2006) 250-259.

[44] N.Y. Topsøe, K. Pedersen, E. G. Derouane, J. Catal. 70 (1981) 41-52.

[45] K. Krishna, M. Makkee, Catal. Lett. 106 (2006) 183-193.

[46] T. K. Katranas, A. G. Vlessidis, V. A. Tsiatouras, K. S. Triantafyllidis, N. P. Evmiridis, Micropor. Mesopor. Mater. 61 (2003) 189-198.

[47] K. Sun, H. Xia, E. Hensen, R. van Santen, C. Li, J. Catal. 238 (2006) 186-95.

[48] P. K. Roy, R. Prins, G. D. Pirngruber, Appl. Catal. A 80 (2008) 226-236.

[49] G. D. Pringruber, P. K. Roy, Catal. Today 110 (2005) 199-210.

[50] Q. Zhu, R. M. van Teeffelen, R. A. van Santen, E. J. M. Hensen, J. Catal. 221 (2004) 575-583.

[51] G. D. Pringruber, P. K. Roy, N. Weiher, J. Phys. Chem. B 108 (2004) 13746-13754.

[52] E. J. M. Hensen, Q. Zhu, R.A. van Santen J. Catal. 220 (2003) 260-264.

[53] E. J. M. Hensen, Q. Zhu, R. A. J. Janssen, P. C. M. M. Magusin, P. J. Kooyman, R. A. van Santen J. Catal. 233 (2005) 123-135.

[54] E. J. M. Hensen, Q. Zhu, R. A.van. Santen, J. Catal., 233 (2005) 136-146.

[55] G. D. Pirngruber, P. K. Roy, R. Prins, J. Catal. 246 (2007) 147-157.

[56] A. Waclaw, K. Nowinska, Stud. Surf. Sci. Catal. 158 (2005) 877-884.

[57] A. Ates, A. Reitzmann, G. Waters, Appl. Catal. B 119- 120 (2012) 329-339.

[58] El-M. El-Malki, R. van Santen, W. Sachtler, J. Phys. Chem. B 103 (1999) 4611–4622.

[59] J. Perez-Ramirez, G. Mul, F. Kapteijn, J. A. Moulijn, A. R. Overweg, A. Domenech, A. Ribera, I. W. C. E. Arend, J. Catal. 207 (2002) 113-126.

[60] J. Bandiera, Y. B. Taarit, Appl. Catal. A 132 (1995) 157-167.

[61] M. C. Abello, M. F. Gomeza, M. Casella, O. A. Ferretti, M. A. Banares, J. L. G. Fierro, Appl. Catal. A 251 (2003) 435-447.

[62] A. V. Kucherov, V. D. Nissenbaum, T. N. Kucherova, L. M. Kustov, Kinetic. Catal. 43(1) (2002) 99-106.

[63] N. A. S. Amin, D. D. Anggora, J. Nat. Gas. Chem. 11 (2002) 79-86.

[64]L. V. Pirutko, V. S. Chernyavsky, A. K. Uriarte, G. I. Panov, Appl. Catal. A 227

(2002)143-157.

Figure and Table Captions

Table 1. XRD crystallinity and chemical composition of Fe-ZSM-5 and Fe-SiO_2 catalysts.

Table 2. Surface characteristics of Fe-ZSM-5 and Fe-SiO_2 prepared by heating at 300 °C under a reduced pressure of 10^{-5} Torr.

Table 3. Percentage weight loss of NH_4-ZSM-5 and Fe-ZSM-5 coked in ODHP with N_2O and/or O_2 with increasing temperature between room temperature and 500 ^oC or 900 ^oC with ramp rate of 10 ^oC /min.

Table 4. Initial ODHP results over Fe-ZSM-5 and Fe-SiO_2 using N_2O, O_2 and N_2O/O_2 mixture after LT treatment

Figure 1. DR-UV-vis spectra of Fe-ZSM-5 zeolites treated at LT, HT and ST and Fe-SiO_2 treated at LT. Parent zeolite and silica were used as references.

Figure 2. NH_3-TPD of NH_4ZSM-5 zeolites after LT and HT treatment (15 (v/v) % NH_3 in He; m_{cat}=0.2 g; F_{total}= 25 $cm^3\,min^{-1}$).

Figure 3. NH_3-TPD of parent zeolites and their iron exchanged forms (15 (v/v) % NH_3 in He; m_{cat}=0.2 g; F_{total}= 25 $cm^3\,min^{-1}$).

Figure 4. NH_3-TPD of Fe-ZSM-5 zeolites treated at LT, HT and ST (15 (v/v) % NH_3 in He; m_{cat}=0.2 g; F_{total}= 25 $cm^3\,min^{-1}$).

Figure 5. NH_3-TPD of SiO_2 and Fe-SiO_2 samples treated at 500 ^oC in He (15 (v/v) % NH_3 in He; m_{cat}=0.2 g; F_{total}= 25 $cm^3\,min^{-1}$).

Figure 6. The conversion of propane (a) and nitrous oxide (b), yield (c) and selectivity (d) of propene as a function of time at 450 ^{o}C over Fe-ZSM-5 zeolites at treated at LT (Feed: 5 (v./v.) % C_3H_8 and 5 (v./v.) % N_2O in He, m_{cat}=0.5 g; Ftotal=200 cm^3 min^{-1}; T=450 ^{o}C)

Figure 7. The conversion of propane (a) and nitrous oxide (b), yield (c) and selectivity (d) of propene as a function of time at 450 ^{o}C over Fe-ZSM-5 zeolites after consecutive ST and HT (Feed: 5 (v./v.) % C_3H_8 and 5 (v./v.) % N_2O in He, m_{cat}=0.5 g; Ftotal=200 cm^3 min^{-1}; T=450 ^{o}C).

Figure 8. Influence of iron content of silica on ODHP performance (Feed: 5 (v./v.) % C_3H_8 and 5 (v./v.) % N_2O in He, m_{cat}=0.5 g; Ftotal=200 cm^3 min^{-1}; T=450 ^{o}C)

Figure 9. Conversion – selectivity plot for the Fe-ZSM-5 catalyst reported in this work and the best results reported in the litterature [2-5, 8, 10] for Fe-ZSM-5 catalysts.

Tables

Table 1. XRD crystallinity and chemical composition of Fe-ZSM-5 and Fe-SiO_2 catalysts.

Samples	Fe (wt.%)	Si/Al ($mol.mol^{-1}$)	Fe/Al ($mol.mol^{-1}$)	[a]Crystal phase
SM27Fe1.0	1.25	12.0	-	ZSM–5
Z23Fe1.0	0.86	11.5	0.13	ZSM–5
Z30Fe1.0	1.0	15.0	-	ZSM–5
Z50Fe1.0	0.93	25.0	0.34	ZSM–5
Z80Fe1.0	1.0	40.0	-	ZSM–5
Z280Fe1.0	1.33	140.0	0.04	ZSM–5
Fe-SiO_2-1 (S1)	0.1	∞	-	Silica
Fe-SiO_2-2 (S2)	0.67	∞	-	Silica
Fe-SiO_2-3 (S3)	0.90	∞	-	Silica

[a] Determined by XRD

Table 2. Surface characteristics of Fe-ZSM-5 and Fe-SiO_2 prepared by heating at 300 °C under a reduced pressure of 10^{-5} Torr.

Samples	S_{BET} (m^2g^{-1})	S_{MP} (m^2g^{-1})	V_{MP} (cm^3g^{-1})		d_{MP} (Å)
			t-plot	DR method	
Z23Fe1.0LT	373	300	0.10	0.14	6.9
Z23Fe1.0HT	346	294	0.12	0.12	7.1
Z23Fe1.0ST	373	326	0.14	0.17	9.8
SM27Fe1.0LT	442	254	0.08	0.16	7.1
SM27Fe1.0HT	334	257	0.10	0.12	7.7
SM27Fe1.0ST	437	281	0.10	0.17	8.7
Z30Fe1.0LT	476	394	0.16	0.19	15.6
Z30Fe1.0HT	396	304	0.12	0.15	9.8
Z30Fe1.0ST	450	373	0.18	0.17	11.6
Z50Fe1.0LT	419	322	0.14	0.22	11.3
Z50Fe1.0HT	253	192	0.09	0.10	12.2
Z50Fe1.0ST	342	276	0.14	0.14	14.4
Z80Fe1.0LT	464	383	0.16	0.19	17.6
Z80Fe1.0HT	332	273	0.14	0.14	14.5
Z80Fe1.0ST	450	373	0.18	0.17	9.4
Z280Fe1.0LT	417	-	-	0.24	30.6
Z280Fe1.0HT	367	207	0.16	0.18	10.4
Z280Fe1.0ST	372	325	0.16	0.14	9.4
Fe-SiO_2-1	373	-	0.12	0.22	27.8
Fe-SiO_2-2	290	n.d	n.d	0.22	31.3
Fe-SiO_2-3	360	n.d	n.d	0.15	31.1

S_{BET}: Multi point BET analysis; S_{MP}: Micropore area determined by t-plot method; V_{MP}: Micropore volume determined by t -plot and DR methods; d_{MP}: Micropore diameter determined by DR method.

Table 3. Percentage weight loss of NH_4-ZSM-5 and Fe-ZSM-5 coked in ODHP with N_2O and/or O_2 with increasing temperature between room temperature and 500 ^oC or 900 ^oC with ramp rate of 10 ^oC /min.

Samples	LT		HT		ST		STHT	
	500^oC	900 ^oC	500^oC	900 ^oC	500^oC	900 ^oC	500^oC	900 ^oC
SM27	10.7	11.6						
Z23	10.5	11.6						
Z30	9.2	9.9						
Z50	7.2	8.0						
Z80	5.8	6.6						
Z280	2.1	2.5	-	-	-	-	-	-
SM27Fe1.0	10.4	11.8	-	-	5.6	7.2	6.6	8.5
Z23Fe1.0	7.9	10.7	-	-			6.3	7.2
Z30Fe1.0	8.2	11.0	-	-			5.4	6.9
Z50Fe1.0	9.5	13.0	-	-			7.1	8.3
Z80Fe1.0	9.0	11.2	8.2	9.6	7.5	9.0	6.0	6.6
Z280Fe1.0	6.0	6.6	-	-	7.9	8.6	5.9	6.7

	LT	HT
Z80Fe1.0(N_2O:C_3H_8=2:1)	9.6	14.2
Z80Fe1.0(N_2O:C_3H_8:O_2=2:1:1)	9.0	14.0
Z80Fe1.0(C_3H_8:O_2=1:1)	9.0	11.8
Z80Fe1.0(O_2:N_2O: C_3H_8=1:1:2)	9.7	14.3

Table 4. Initial ODHP results over Fe-ZSM-5 and Fe-SiO_2 using N_2O, O_2 and N_2O/O_2 mixture after LT treatment.

Samples	$C_3H_8/N_2O/O_2$ (% vol.)	T (^oC)	X_{C3H8} (%)	S_{C3H6} (%)	Y_{C3H6} (%)
SM27Fe1.0	5/5/-	450	9.50	62.8	5.9
Z23Fe086	5/5/-	450	39.0	17.0	6.0
Z30Fe1.0	5/5/-	450	33.0	20.0	7.0
Z50Fe0.90	5/5/-	450	29.0	19.0	5.0
Z80Fe1.0	5/5/-	450	28.0	21.0	6.0
Z280Fe1.0	5/5/-	450	25.0	39.0	9.8
Z280Fe1.0	5/5/-	500	23.8	73.2	17.4
Z280Fe1.0	5/-/5	500	2.4	57.6	2.0
Z80Fe1.0	5/-/5	500	3.0	89.2	2.6
Z80Fe1.1	5/2.5/2.5	500	15.8	81.8	12.8
Z80Fe1.0	**5/10/-**	**500**	**29.2**	**68.8**	**20.0**
Z80Fe1.1	5/10/5	500	14.9	88.9	13.2
Z80Fe1.0	5/5/-	450	14.6	75.4	11.0
$FeSiO_2$-1	5/5/-	450	1.1	96.6	1.0
$FeSiO_2$-2	5/5/-	450	3.8	97.6	3.9
$FeSiO_2$-2	5/5/-	500	3.8	98.8	5.7
$FeSiO_2$-3	5/5/-	450	4.6	98.6	4.6
$FeSiO_2$-3	5/-/5	450	3.1	89.3	2.8
$FeSiO_2$-3	5/10/-	450	4.9	97.9	4.8
$FeSiO_2$-3	**5/5/5**	**450**	**7.9**	**89.8**	**7.2**

FIGURES

Figure 1.

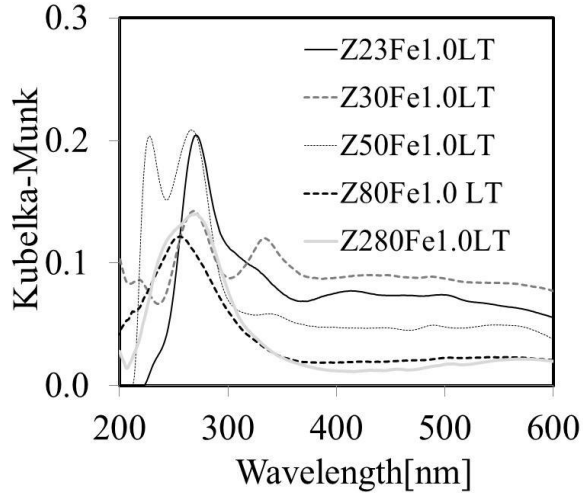

(a)

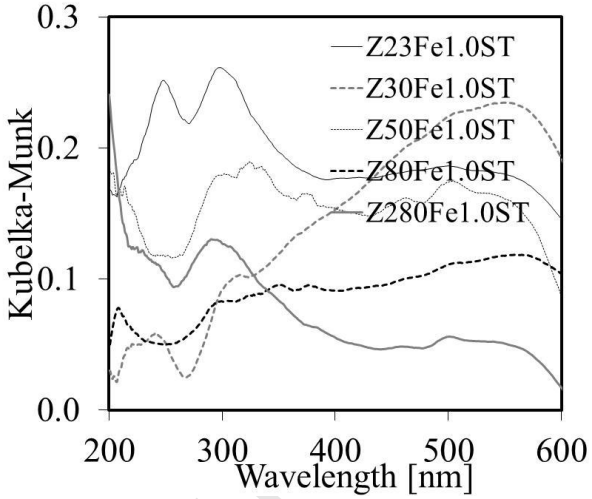

(b)

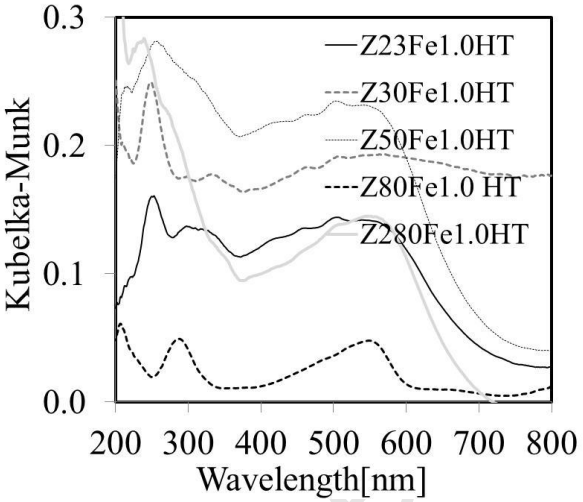

(c)

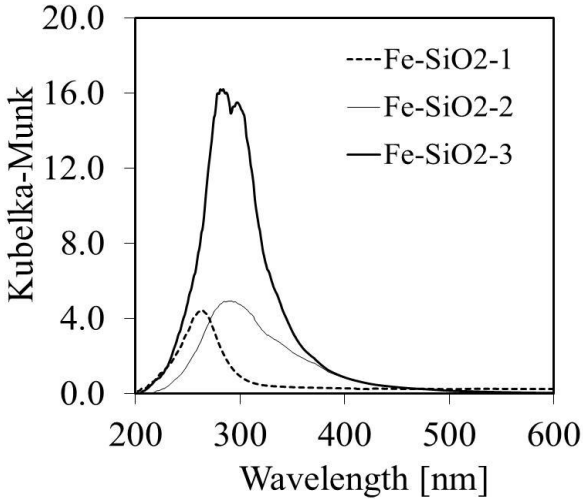

(d)

Figure 2.

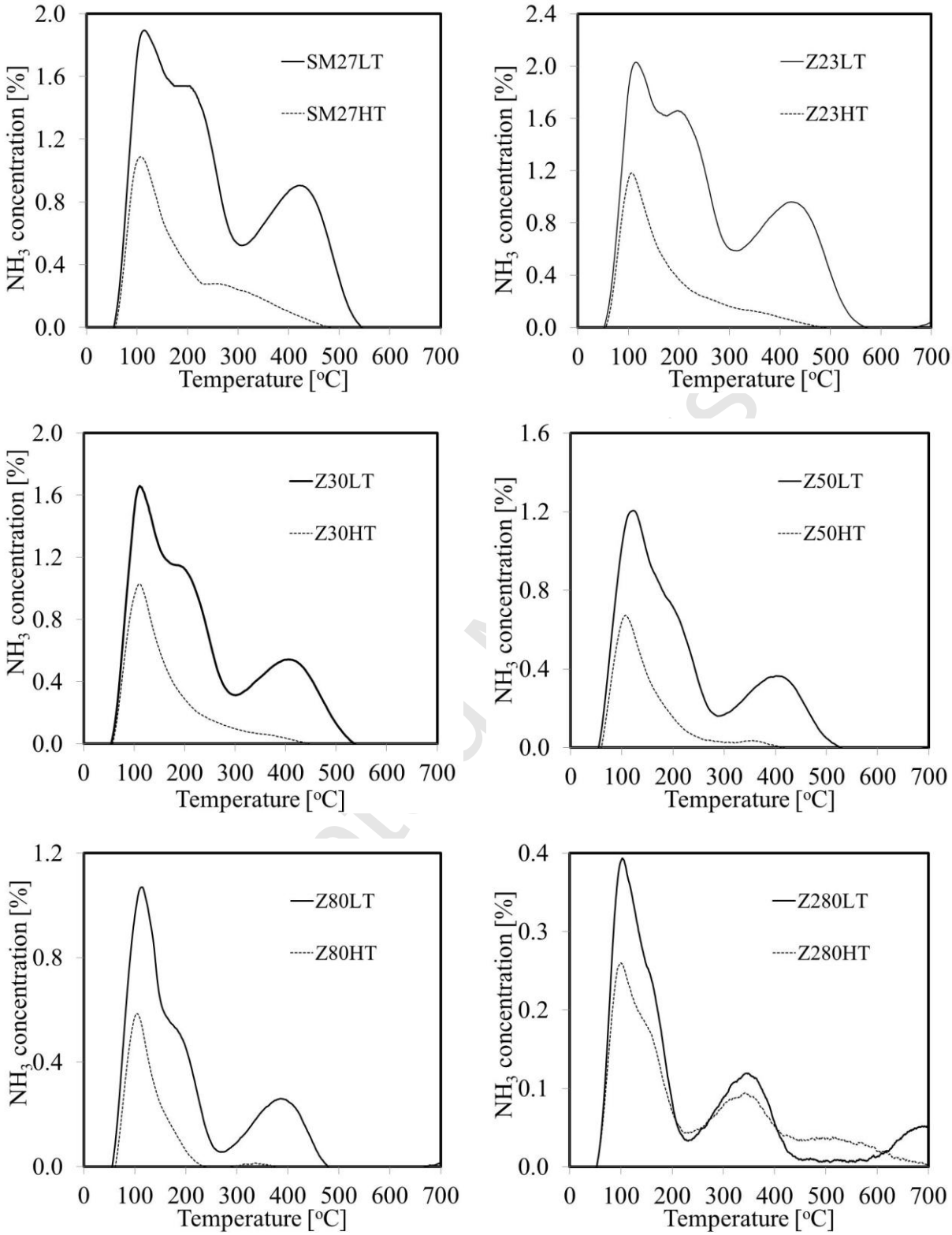

Figure 3.

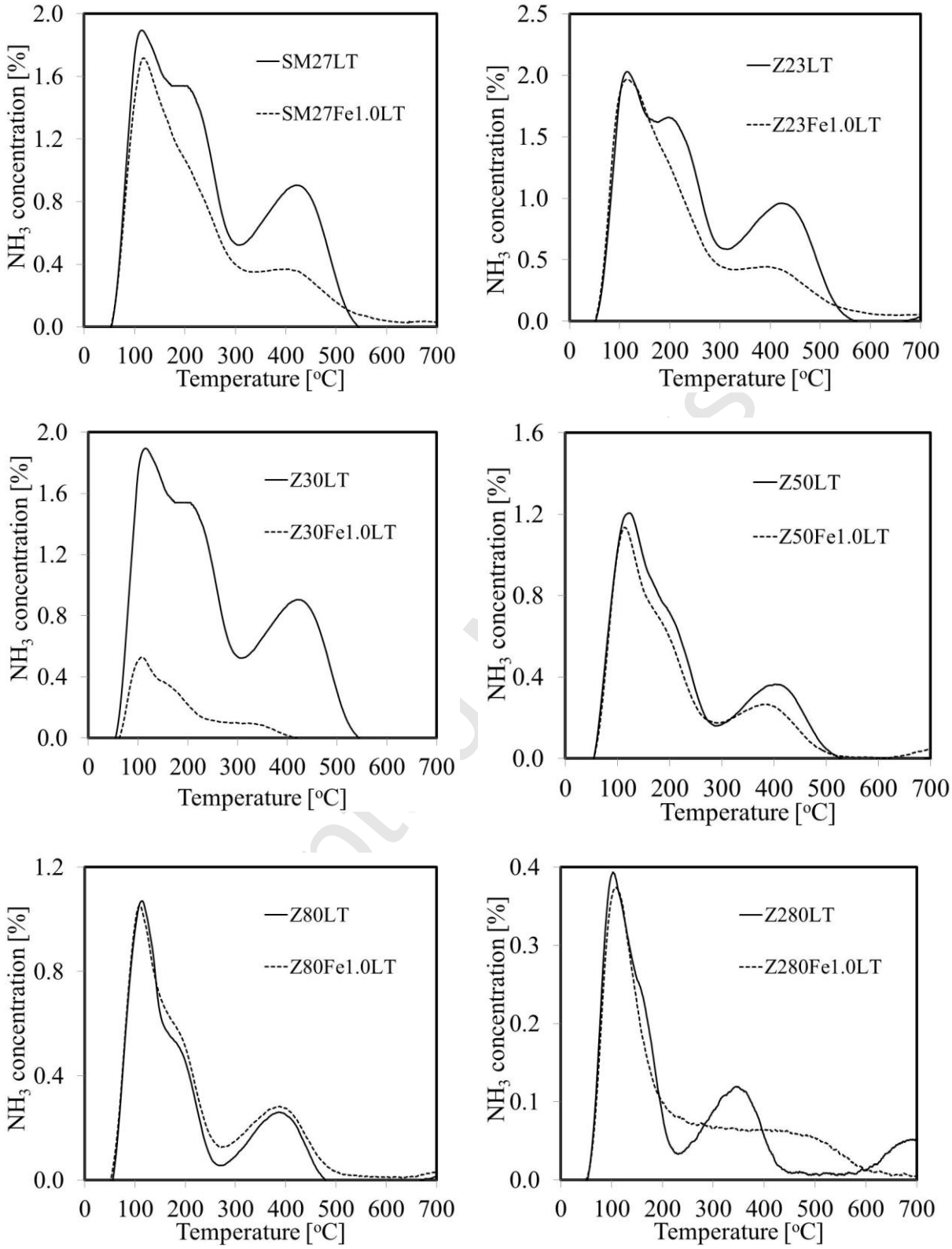

Figure 4.

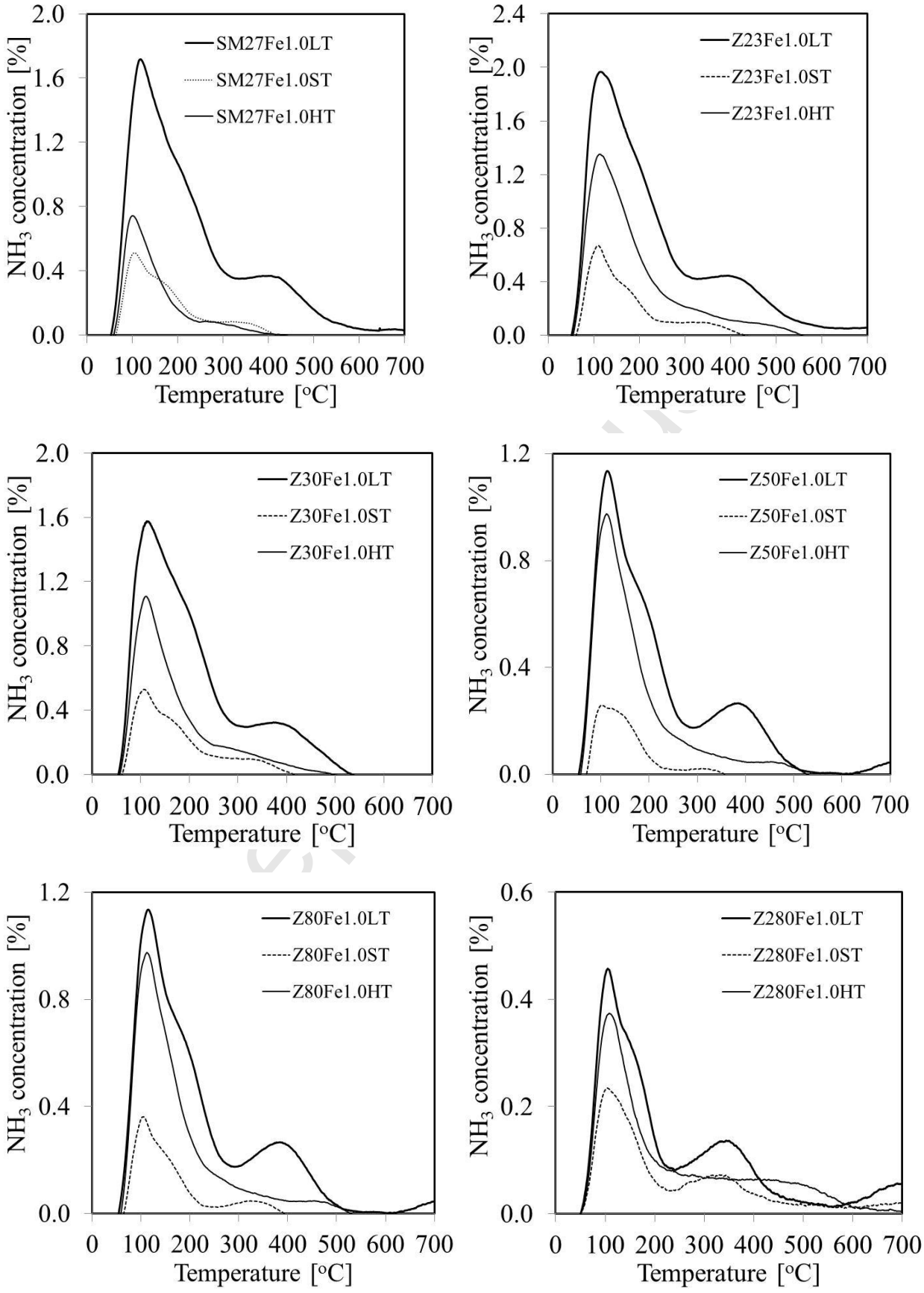

Figure 5.

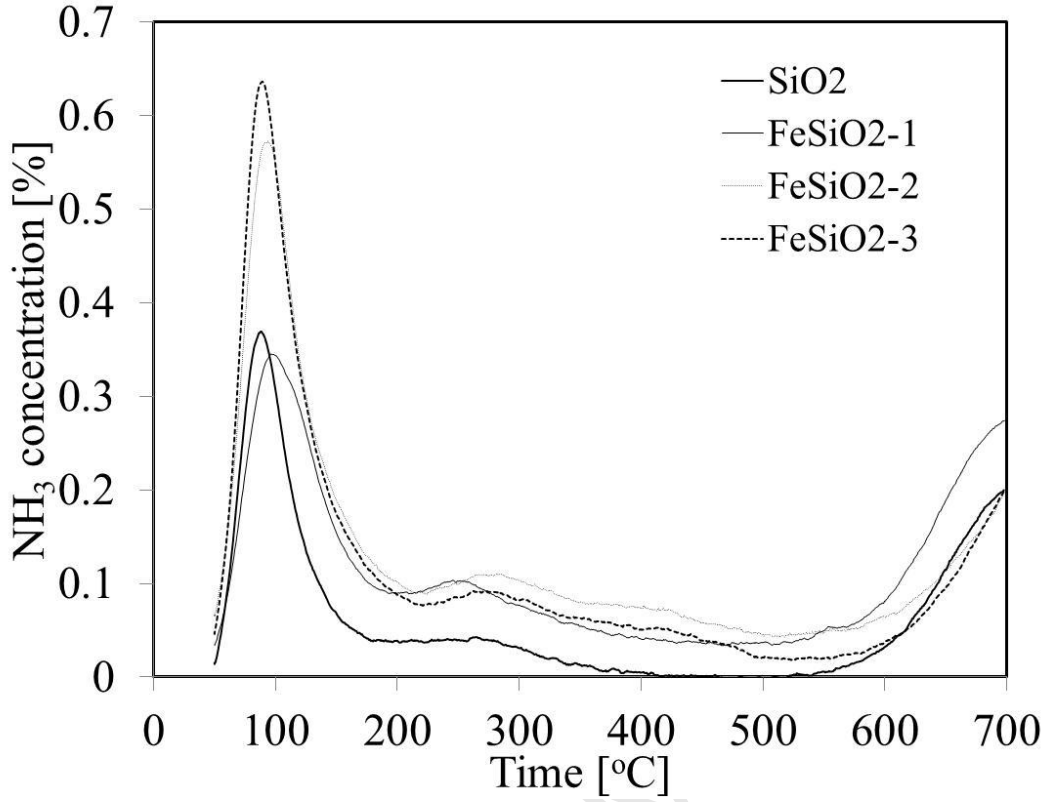

Figure 6.

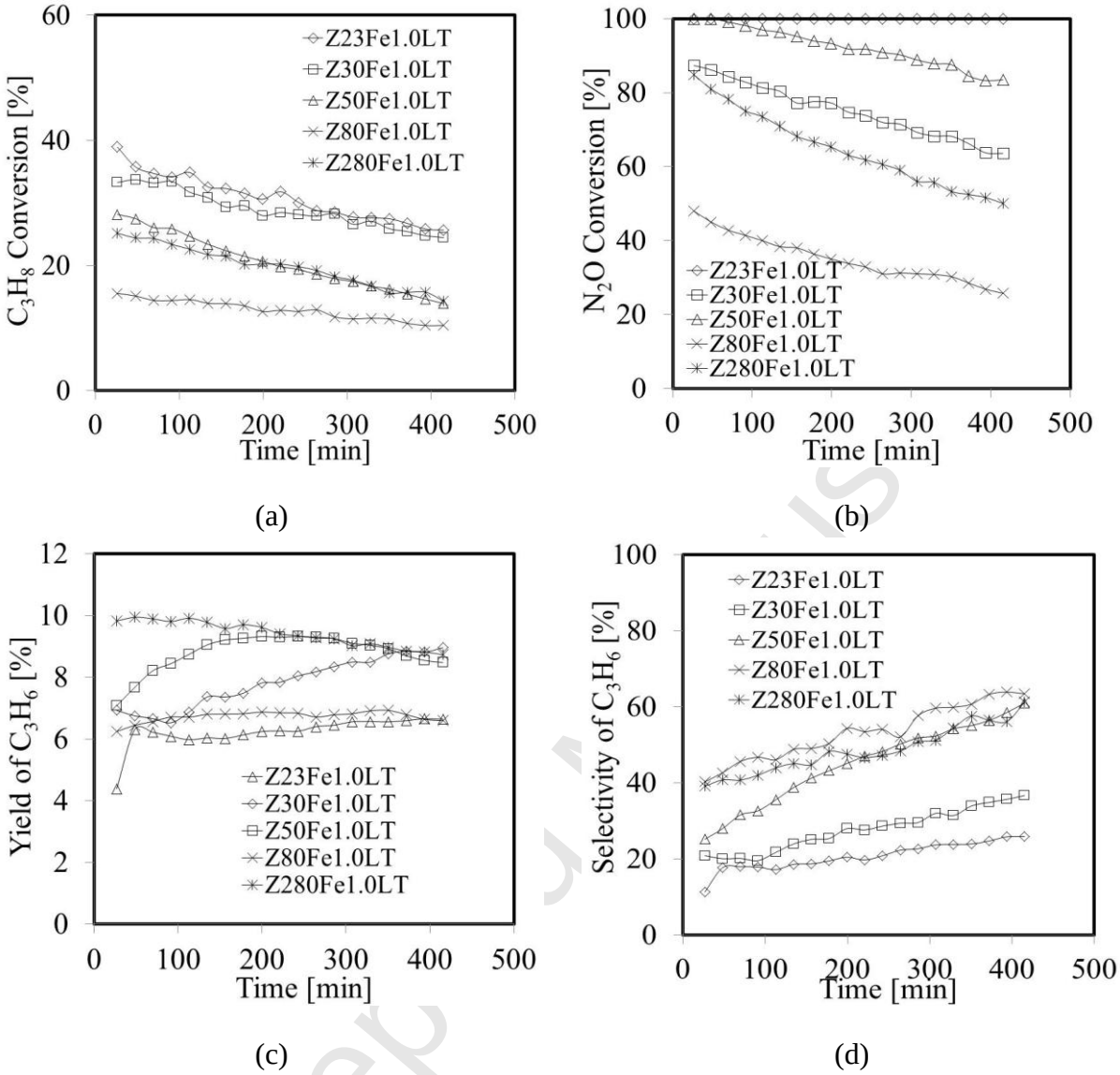

Figure 7.

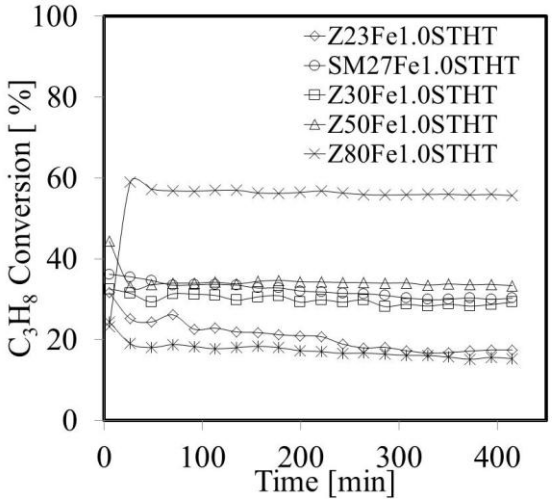

(a)

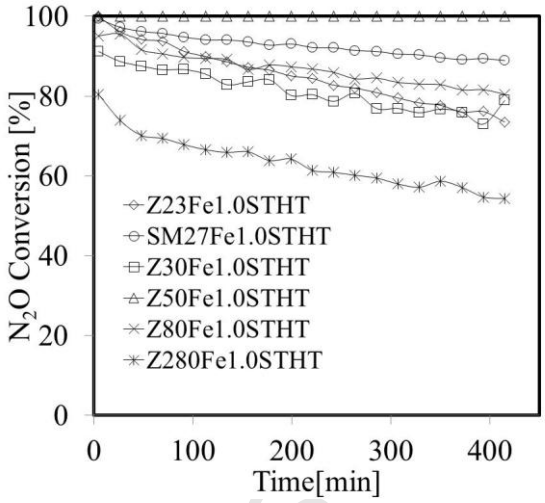

(b)

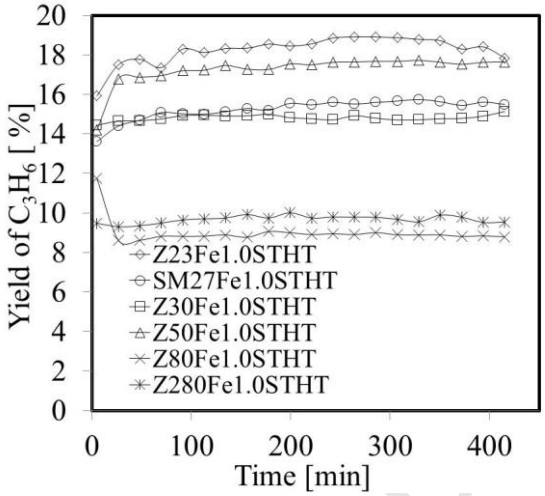

(c)

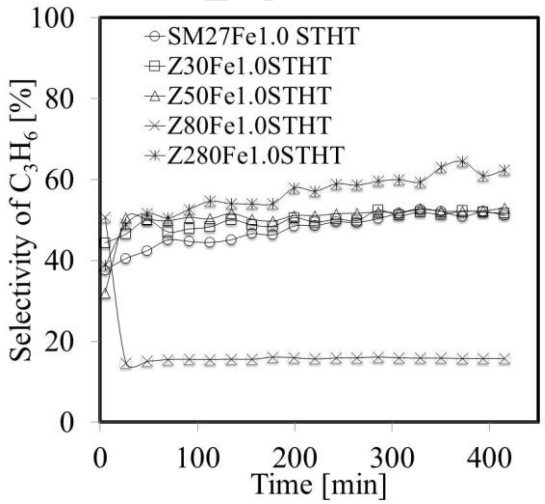

(d)

Figure 8.

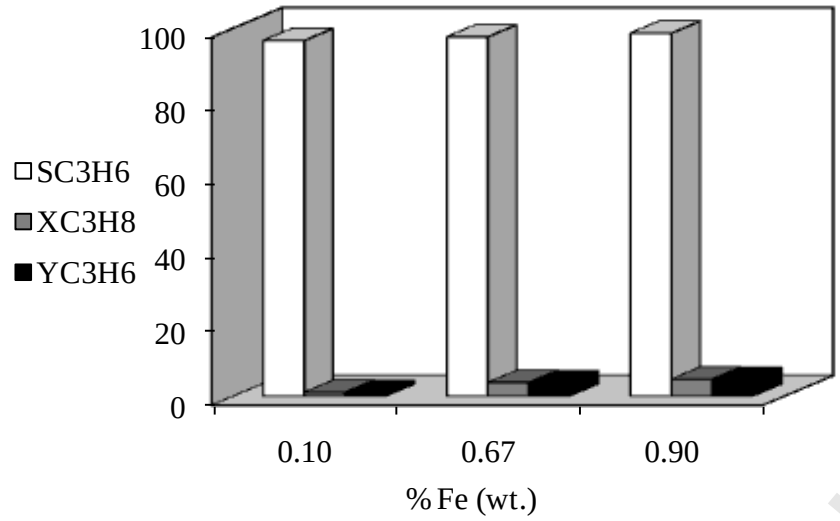

Figure 9.